Eur. Phys. J. E (2004)
DOI 10.1140/epje/i2004-10002-8

THE EUROPEAN PHYSICAL JOURNAL E

Impact craters in loose granular media

X.-J. Zheng, Z.-T. Wang[a], and Z.-G. Qiu

Department of Mechanics, Lanzhou University, Lanzhou, 730000, PRC

Received 14 February 2004 and Received in final form 16 March 2004 /
Published online: 6 April 2004 –

Abstract. The craters formed by the impact of steel balls with a loose sand bed are experimentally studied. Both crater size and morphology depend strongly on the impact angle. Two scaling laws, corresponding to length and width, respectively, are proposed.

PACS. 45.70.-n Granular systems – 83.80.Fg Granular solids

Craters exist on Mars, the Earth, and other planets with solid surface. As "written" record of impact events, craters have been of fundamental interest among geophysicists [1–4]. It is possible to estimate the threat of asteroids to the Earth provided that the impact process is completely revealed. Two very recent experiments [5, 6] on impact craters formed by dropping a ball vertically into a container of granular material suggest that many important aspects of large-scale crater formation can be meaningfully modelled in low-energy laboratory experiments on granular media, although a detailed analogy may be limited. The crater diameter is confirmed to scale as the $\frac{1}{4}$ power of the impact energy. However, natural impacts take place over a variety of angles and the crater shape is not always circular [7–11].

Here we focus on the influence of the impact angle on the crater morphology and size. The experimental apparatus and procedures are as follows. A device with 2 m long stainless-steel groove with a semicircular cross-section was designed. The inner/outer diameter is 1.9 cm/2.5 cm. The inclination angle, θ, of the groove can be changed. A 90 cm long, 20 cm wide and 8.3 cm deep container of naturally mixed, dry and noncohesive quartz sand is placed under the lower end of the groove. The analysis of sand diameter has been performed by Zhou *et al.* [12]. The mean size of grains is 0.228 mm. The volume fraction of the granular medium has a great effect on the crater formation. To keep the same initial state of sand bed, a special treatment is adopted before each test. At first, the sand is stirred up. The generated sandpiles are slightly higher than the container edges which are very straight and smooth. Then, a rigid ruler is slowly pushed along the two longer edges of the container. Some sand grains flow out during this process. Finally, a small silo is used to add sand to a few places which are lower than the container edge. The mass difference between the added and lost sand is less than 0.250 kg. As a comparison, the total sand in the container exceeds 15 kg. The added sand is also smoothed by the ruler. Now the sand bed is almost loose and flat everywhere. The noticeable defects are further repaired by lightly tapping or blowing. In the experiment, a steel ball, ranging from 0.40 cm to 1.83 cm in diameter, is released with zero speed from a site of the groove. It will collide with the sand bed after rolling a distance, h, along the groove. The total energy dissipation due to the friction between the ball and the inner surface of the groove cannot reach 3% of the ball's potential energy or $mgh\sin\theta$. When the ball comes to rest, we begin to observe the crater. To reduce the influences of the container edge and the lower end of the groove, the impact site is kept near the center of the container and a distance of about 2.5 mm between the surface of the sand bed and the groove is needed. We vary θ from 10° to 80°, h from 10 cm to 200 cm. For vertical impacts, a like method as described in [5, 6] is applied.

As pointed out in previous studies [7, 8, 13], the resultant crater depends on many factors. The crater shape is jointly determined by the release site, the ball diameter and the impact angle, etc., in this experiment. The impacte angle plays a dominating role. For example, although other factors may be greatly different, all craters are circular when $\theta = 90°$. So we can make a rough classification of crater morphology in the light of the impact angle, see Figure 1. i) For large impact angles ($70° \lesssim \theta \leqslant 90°$), craters are often circular. A simple crater (Fig. 1(a)) is the most familiar sight. We also find a circular crater with a small central peak (Fig. 1(b)). But the complex crater seen by Walsh *et al.* [6] does not exist in our experiments since the cohesive forces between grains are very weak for the granular medium we used. ii) For medium impact angles ($40° \lesssim \theta \lesssim 70°$), an elliptical crater, which has never been investigated in previous experiments on low-energy impacts, appears. Unlike the

[a] e-mail: wangzht02@st.lzu.edu.cn

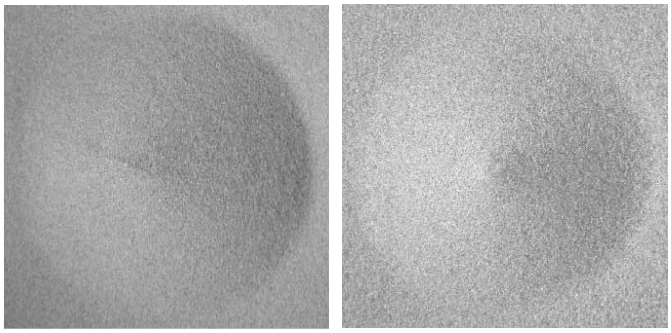

(a) simple crater

(b) crater with a central peak

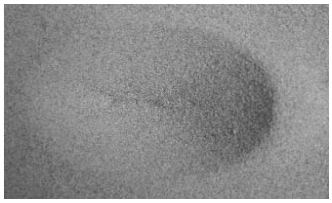

(c) elliptical crater

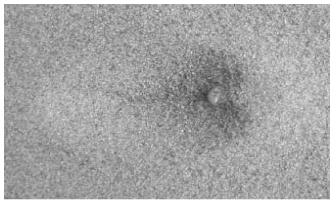

(d) crater with the ball exposed

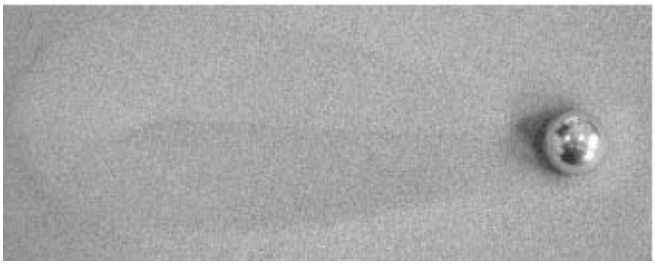

(e) triangular crater

Fig. 1. Typical craters.

uniform rim of the simple crater, the lowest or highest location of the rim occurs on the prolate axis of the ellipse for this type of craters. In most cases, the ball is buried completely (Fig. 1(c)). While Figure 1(d), in which the ball is exposed partly, indicates that the ball will move a distance after the impact. The sand is pushed outwards and forward. This process leads to the formation of an elliptical crater. iii) For small impact angles ($\theta \lesssim 40°$), the typical crater configuration (Fig. 1(e)) is distinctly different from that depicted above. It looks like an acute triangle or a tadpole. A similar scenery of crater morphologies as shown in Figures 1(a) and (c) is observed on many planets. A detailed comparison of circular craters between laboratory and planetary has been performed by Walsh *et al.* [6]. From a mathematical point of view, the elliptical crater can be well identified with eccentricity rather than

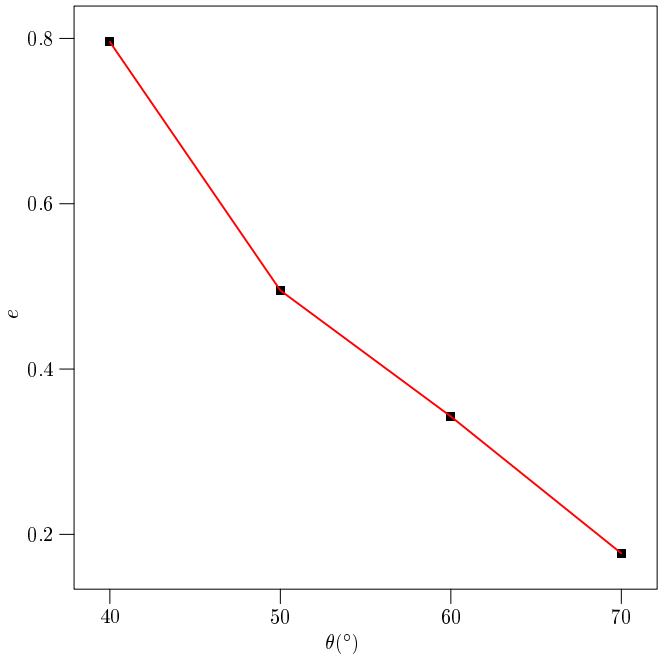

Fig. 2. Eccentricity of an elliptical crater *versus* impact angle.

with the "ellipticity" defined by Bottke *et al.* [11]. After averaging eccentricities of all craters at certain impact angles, we find that eccentricity increases with decreasing impact angle, see Figure 2. This tendency is in accord with the results of hypervelocity experiments [7,14]. The mean eccentricity of 223 Martian elliptical craters classified as "Likely" and "Possible" in reference [11] is calculated. This value (= 0.71) is included in our experimental results (Fig. 2).

Now let us consider the scaling laws for the crater size. The release site, h, the ball diameter, d, and the grain size, $d_{\rm g}$, are three relevant length scales. As far as we know, $d_{\rm g}$ plays a fundamental role in two situations. When $d \sim d_{\rm g}$, the impacting ball may rebound from the granular bed and eject a few grains [13,15]. The crater could have the same length scale as a single grain in this case. For very small grains ($d_{\rm g} \lesssim 0.090\,$mm in Ref. [6]), cohesive forces directly exert an influence on crater formation. Since $d \gg d_{\rm g}$ and $d_{\rm g} \approx 0.228\,$mm in this experimental study, the effect of grain size is insignificant, as compared with that of h and d. So, it seems that the simplest forms of crater size are

$$l = C_l d^{\alpha} h^{1-\alpha}\,, \tag{1}$$

$$w = C_w d^{\beta} h^{1-\beta}\,, \tag{2}$$

where l and w, both defined by the location of the maximum rim height, are the crater length and width, respectively. If the width is not a constant in the direction of the impact (as in Fig. 1(e)), the measured maximum value is defined as the crater width. Given an impact angle, θ, the nondimensional coefficients, C_l and C_w, and the exponents, α and β, can be obtained by using the least-squares method. Figure 3, in which only the data for $\theta = 40°$, $60°$

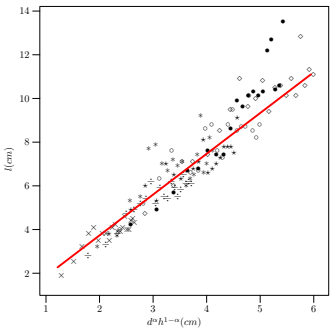

(a) $\theta = 40°$, $C_l = 1.87$, $\alpha = 0.75$

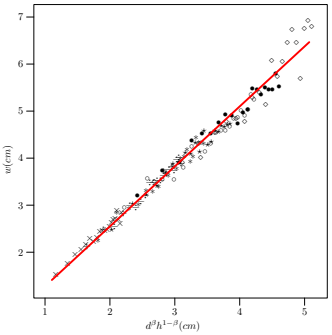

(b) $\theta = 40°$, $C'_w = 1.98$, $\beta = 0.78$

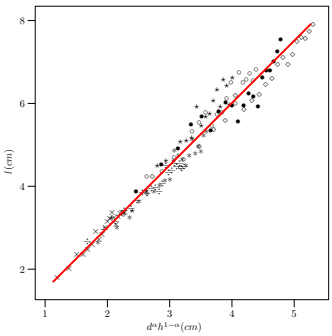

(c) $\theta = 60°$, $C_l = 1.50$, $\alpha = 0.77$

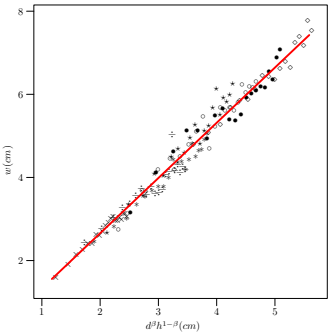

(d) $\theta = 60°$, $C'_w = 1.53$, $\beta = 0.76$

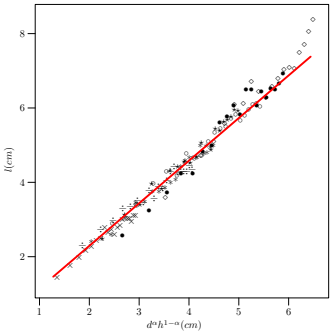

(e) $\theta = 80°$, $C_l = 1.15$, $\alpha = 0.73$

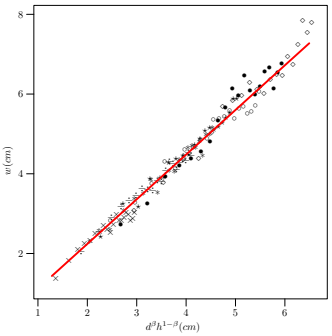

(f) $\theta = 80°$, $C'_w = 1.14$, $\beta = 0.73$

Fig. 3. Scaling of the crater size with ball diameter and release site: $\times$ for $d = 0.60$ cm, $\div$ for $d = 0.95$ cm, $*$ for $d = 1.10$ cm, $\star$ for $d = 1.27$ cm, $\circ$ for $d = 1.43$ cm, $\bullet$ for $d = 1.60$ cm, $\diamond$ for $d = 1.83$ cm, solid lines for predictions of equations (1) and (2).

and 80° are plotted and $C'_w = \frac{C_w}{\sin\theta}$, shows that equations (1) and (2) agree well with experimental results. C_w is normailzed by $\sin\theta$ for the convenience of further data treatment.

It is found that the coefficients and exponents in the above scaling laws are not constants in the whole range of

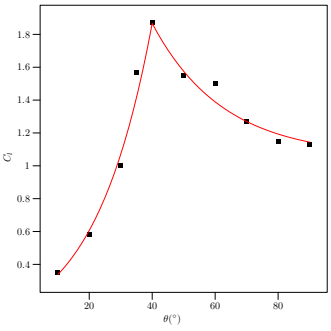

(a) C_l as a function of θ

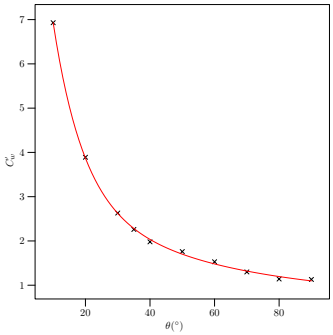

(b) C'_w as a function of θ

Fig. 4. Coefficient *versus* impact angle: ■ and $\times$ for the data obtained by the least-squares method, solid lines for predictions of equations (3) and (4).

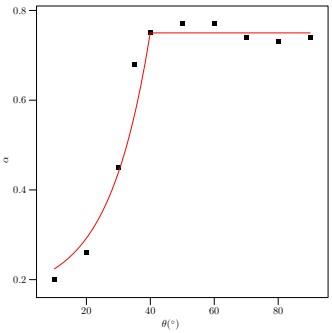

(a) α as a function of θ

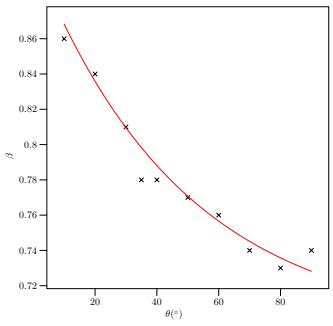

(b) β as a function of θ

Fig. 5. Exponent *versus* impact angle: ■ and $\times$ for the data obtained by the least-squares method, solid lines for predictions of equations (5) and (6).

impact angle. The fitted expressions are as follows:

$$C_l = \begin{cases} -0.03631 + 0.21691\exp(\theta/0.32145), & \theta \le \theta_0, \\ 1.05722 + 4.81566\exp(-\theta/0.39149), & \theta > \theta_0, \end{cases} \quad (3)$$

$$C'_w = \begin{array}{l} 0.70089 + 2.81827\exp(-\theta/0.80073) \\ +11.67266\exp(-\theta/0.16161), \end{array} \quad (4)$$

$$\alpha = \begin{cases} 0.16433 + 0.0279\exp(\theta/0.22920), & \theta \le \theta_0, \\ 0.75, & \theta > \theta_0, \end{cases} \quad (5)$$

$$\beta = 0.69528 + 0.21284\exp(-\theta/0.84159), \quad (6)$$

where $\theta_0 \approx \frac{2}{9}\pi$ (or 40 in degrees). The comparisons between the fitting curves and the experimental data are given in Figures 4 and 5. The $\frac{1}{4}$ power law, which has been established when $\theta = 90°$ [5, 6], is still valid to describe the crater length for large impact angles. But such a simple law fails for the width scale and all cases of small

impact angles. Both C_l and α in length scaling will increase with θ until the morphology of the crater changes obviously, or the elliptical crater appears, and then C_l decreases, α remains a constant (about 0.75). C'_w and β are all decreasing functions of θ.

In summary, we have systematically investigated the crater morphology and measured the crater length and width. For large and medium impact angles, striking similarities are seen in laboratory and planetary crater morphologies. Based on experimental data, two scaling laws are proposed and the applicability of $\frac{1}{4}$ power law is given. The present work suggests that the behaviour of a granular medium under the oblique impact of a hard object is very interesting. The dependence of crater formation on the impacting material properties, the volume fraction and cohesive forces of granular media, planetary gravity and atmospheric parameters, etc., should be further studied in detail. Theoretical description and numerical simulation of the observed phenomenon are also needed.

Z.-T. Wang is grateful to Dr. You-He Zhou for valuable discussions, to Mr. Shou-San Li for his help in the design and construction of experimental setup. This research was supported by the National Key Basic Research and Development Foundation of the Ministry of Science and Technology of China No. G2000048702.

References

1. K.R. Housen, R.M. Schmidt, K.A. Holsapple, J. Geophys. Res. **88**, 2485 (1983).
2. H.J. Melosh, *Impact Cratering: A Geologic Process* (Oxford University Press, New York, 1989).
3. K.A. Holsapple, Annu. Rev. Earth Planet. Sci. **21**, 333 (1993).
4. B.J. Gladman, J.A. Burns, M. Duncan, P. Lee, H.F. Levison, Science **271**, 1387 (1996).
5. J.S. Uehara, M.A. Ambroso, R.P. Ojha, D.J. Durian, Phys. Rev. Lett. **90**, 194301 (2003).
6. A.M. Walsh, K.E. Holloway, P. Habdas, J.R. de Bruyn, Phys. Rev. Lett. **91**, 104301 (2003).
7. D. Gault, J. Wedekind, *Proceedings of the ninth Lunar and Planetary Science Conference Publication* (Pergamon Press, 1978) p. 3843.
8. P. Schultz, J. Geophys. Res. **97**, 16183 (1992).
9. H.J. Melosh, I.V. Nemchinov, Yu. I. Zetzer, in *Hazards due to Comets and Asteroids*, edited by T. Gehrels (The University of Arizona Press, 1994).
10. E. Pierazzo, H.J. Melosh, Annu. Rev. Earth Planet. Sci. **28**, 141 (2000).
11. W.F. Bottke, S.G. Love, D. Tytell, T. Glotch, Icarus **145**, 108 (2000).
12. Y.-H. Zhou, X. Guo, X.-J. Zheng, Phys. Rev. E **66**, 021305 (2002).
13. Y. Grasselli, H.J. Herrmann, Gran. Matter **3**, 201 (2001).
14. E.L. Christiansen, E.D. Cytowski, J. Ortega, Int. J. Impact Eng. **14**, 157 (1993).
15. F. Rioual, A. Valance, D. Bideau, Phys. Rev. E **62**, 2450 (2000).